

Importance of exchange anisotropy and superexchange for the spin-state transitions in $R\text{CoO}_3$ ($R = \text{rare earth}$) cobaltates

Guoren Zhang,¹ Evgeny Gorelov,¹ Erik Koch,^{2,3} and Eva Pavarini^{1,3}¹*Institute for Advanced Simulation, Forschungszentrum Jülich, D-52425 Jülich, Germany*²*German Research School for Simulation Sciences, 52425 Jülich, Germany*³*JARA High-Performance Computing*

(Received 2 August 2012; published 12 November 2012)

Spin-state transitions are the hallmark of rare-earth cobaltates. In order to understand them, it is essential to identify all relevant parameters which shift the energy balance between spin states and determine their trends. We find that Δ , the e_g - t_{2g} crystal-field splitting, increases by ~ 250 meV when increasing pressure to 8 GPa and by about 150 meV when cooling from 1000 K to 5 K. It changes, however, by less than 100 meV when La is substituted with another rare earth. Moreover, the Hund's rule coupling \mathcal{J}_{avg} is about the same in systems with very different spin-state transition temperature, like LaCoO_3 and EuCoO_3 . Consequently, in addition to Δ and \mathcal{J}_{avg} , the Coulomb-exchange anisotropy $\delta\mathcal{J}_{\text{avg}}$ and the superexchange energy gain δE_{SE} play a crucial role and are comparable with spin-state-dependent relaxation effects due to covalency. We show that in the LnCoO_3 series, with $\text{Ln} = \text{Y}$ or another rare earth (RE), superexchange progressively stabilizes a low-spin ground state as the Ln^{3+} ionic radius decreases. We give a simple model to describe spin-state transitions and show that, at low temperature, the formation of isolated high-spin/low-spin pairs is favored, while in the high-temperature phase, the most likely homogeneous state is high spin rather than intermediate spin. An *orbital-selective* Mott state could be a fingerprint of such a state.

DOI: [10.1103/PhysRevB.86.184413](https://doi.org/10.1103/PhysRevB.86.184413)

PACS number(s): 71.27.+a, 71.30.+h, 72.80.Ga, 71.10.-w

I. INTRODUCTION

The nature of the spin-state transitions in LaCoO_3 (Fig. 1) has been the subject of controversy for decades.^{1–20} LaCoO_3 undergoes two electronic crossovers, (at $T_{\text{SS}} \sim 50$ –100 K and $T_{\text{IM}} \sim 500$ –600 K); the first is commonly ascribed to a change in spin state, while the second is commonly ascribed to an insulator-to-metal transition.^{2,6} There is a general agreement that the ground state of LaCoO_3 is insulating and nonmagnetic, with Co in the low-spin (LS) t_{2g}^6 state. The core of the debate is whether the $t_{2g}^4 e_g^2$ high-spin (HS) state^{1–5} ($S = 2$) or the $t_{2g}^5 e_g^1$ intermediate-spin (IS) state^{9–15} ($S = 1$) is thermally excited right above T_{SS} and if the spin-state crossover involves two or more steps between T_{SS} and T_{IM} . Various mixed phases^{16,17} and spin-state superlattices^{18–21} have been suggested as final or intermediate step. For the high-temperature phase, a pure IS state has been proposed based on LDA+ U results¹⁷ or phenomenological thermodynamic analysis.²² To date, the controversy remains open.

Spin-state transitions have also been reported in LaCoO_3 under pressure,^{23–26} as well as in several LnCoO_3 perovskites, where Ln is Y or another rare earth (RE) heavier than La.^{27–29} In the LnCoO_3 series, the spin-state and, to a smaller extent, the insulator-to-metal transition, shifts to higher temperatures with decreasing R^{3+} ionic radius.^{27–30} Since HS and IS states are Jahn-Teller (JT) active, one might expect cooperative JT distortions in correspondence with the spin-state transition. Remarkably, early neutron diffraction data^{31–33} indicate that the structure of LaCoO_3 is rhombohedral (space group $R\bar{3}c$) with no cooperative JT distortion at all,^{5,31–33} while, more recently, a cooperative JT distortion (space group $I2/a$) has been found via single-crystal x-ray diffraction.^{14,34} The presence of local JT distortions is as controversial.^{5,35} On the other hand, LnCoO_3 perovskites with $\text{Ln} \neq \text{La}$ are

orthorhombic (space group $Pbnm$) and do exhibit a small, weakly temperature-dependent, JT distortion.^{27,28,30}

The LS \rightarrow IS scenario⁹ was popularized by total-energy LDA+ U calculations,¹² which show that for rhombohedral LaCoO_3 the homogeneous IS state is almost degenerate with the LS ground state and sizably lower in energy than the HS state.^{12,17–19} The LS \rightarrow IS scenario has been used to interpret experiments pointing to a spin triplet.^{11,14,28} However, a triplet can also arise from the splitting of the HS state via spin-orbit interaction.^{13,36,37} Furthermore, it has been shown with LDA+ U and unrestricted Hartree-Fock that some inhomogeneous LS/HS phases and/or superlattices,^{17–19} are more stable than the homogeneous IS state. Experimentally, neither the HS+LS nor other superlattices have been reported so far; instead, there are strong indications that x-ray absorption spectroscopy (XAS) and magnetic circular dichroism (MCD) data³ as well as inelastic neutron scattering experiments⁴ are compatible with a mixed HS/LS phase. It has been pointed out that the lattice could play a crucial role in such mixed phases, by expanding around HS ions due to covalency effects.^{1,3,22}

While the experimental evidence in favor of LS \rightarrow HS crossover at T_{SS} , perhaps with disorder phenomena, is growing,^{3,4,11} the actual parameters which tip the energy balance in favor of a given spin-state in the real materials have not been fully identified, and, to the best of our knowledge, no systematic attempt to determine their evolution in the LnCoO_3 series exist. Furthermore, the interplay between the spin-state and insulator-to-metal transition, even in the simplest homogeneous scenarios, and the nature of the high-temperature metallic phase, are not fully understood.

In the present work, we study the electronic structure trends of the LnCoO_3 family and identify the material-dependent parameters responsible for the spin-state transitions. We show

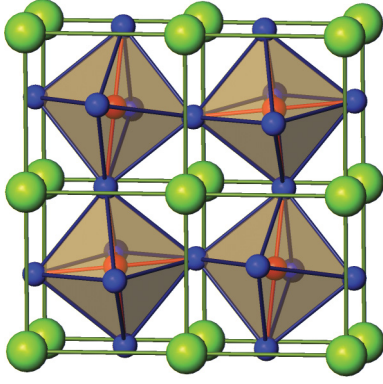


FIG. 1. (Color online) Rhombohedral structure of LaCoO_3 . We define the x , y , z pseudocubic axes as those connecting the Co atoms; z is the vertical axis, y the horizontal axis, and x is perpendicular to the plane of the figure. (Green spheres) La atoms. (Blue spheres) O atoms. (Red spheres) Co atoms.

that, for realistic Coulomb and exchange parameters, an IS homogeneous phase is very unlikely in any of the considered materials, both at low and high temperatures. We show that, besides the interplay of the e_g - t_{2g} crystal-field Δ and the Coulomb exchange \mathcal{J}_{avg} , the exchange anisotropy $\delta\mathcal{J}_{\text{avg}}$ and the superexchange energy gain δE_{SE} play a crucial role. Our results support a scenario in which HS-LS pairs, the formation of which is favored by both superexchange interaction and covalency effects, are excited at T_{SS} . We find that, for all known experimental structures, the Jahn-Teller crystal-field splitting is weak. In the high-temperature regime, we find, within a homogeneous scenario, a HS state; in such a state, the insulator-to-metal transition depends mostly on the t_{2g} degrees of freedom. Our results could be used to distinguish a pure high-temperature HS state from a mixed HS/LS state.

II. METHOD

We calculate the electronic structure using two *ab initio* approaches based on density-functional theory in the local-density approximation (LDA). The first is the linear augmented plane wave (LAPW) method as implemented in the WIEN2K code³⁸; to obtain hopping integrals and crystal-field splitting, we use maximally localized Wannier functions.³⁹ The second approach is the downfolding technique based on the N th-order muffin-tin orbital (NMTO) method in the form discussed in Ref. 40. By means of these two methods, we construct the generalized Hubbard model for the Co d bands,

$$H = - \sum_{im,i'm'\sigma} t_{m,m'}^{i,i'} c_{im\sigma}^\dagger c_{i'm'\sigma} + \frac{1}{2} \sum_{i\sigma,\sigma'} \sum_{mm'} \sum_{pp'} U_{mpm'p'} c_{im\sigma}^\dagger c_{ip\sigma'}^\dagger c_{i'p'\sigma'} c_{im'\sigma}. \quad (1)$$

Here $c_{im\sigma}^\dagger$ creates an electron with spin σ in the Wannier orbital m at site i ($m = xz, yz, xy, x^2 - y^2, 3z^2 - r^2$). $U_{mpm'p'}$ are rotationally invariant screened Coulomb integrals. The parameters $U_{mpm'p'}$ can all be expressed as a function of the

(screened) Slater integrals F_0 , F_2 , and F_4 . We adopt the common definition for the average direct and exchange couplings, $U_{\text{avg}} = F_0$, and $J_{\text{avg}} = \frac{1}{14}(F_2 + F_4)$. A pedagogical derivation of the rotationally invariant Coulomb matrix can be found, e.g., in Ref. 41. Apart from the average exchange interaction, the exchange anisotropy plays a significant role. It is, therefore, convenient to express all parameters as linear combinations⁴² of U_{avg} , $\mathcal{J}_{\text{avg}} = \frac{5}{7}J_{\text{avg}}$, and $\delta\mathcal{J}_{\text{avg}} = \mathcal{J}_{\text{avg}}(\frac{1}{5} - \frac{1}{9}\frac{F_4}{F_2})/(1 + \frac{F_4}{F_2})$; the latter measures the anisotropy in the exchange interactions. The exchange parameters for the t_{2g} and e_g states are then $J_{t_{2g}} = \mathcal{J}_{\text{avg}} + \delta\mathcal{J}_{\text{avg}}$ and $J_{e_g} = \mathcal{J}_{\text{avg}} + 3\delta\mathcal{J}_{\text{avg}}$, respectively; the Coulomb exchange parameters between e_g and t_{2g} states are $J_{3z^2-r^2,xz} = J_{3z^2-r^2,yz} = \mathcal{J}_{\text{avg}} - 3\delta\mathcal{J}_{\text{avg}}$, $J_{x^2-y^2,xy} = \mathcal{J}_{\text{avg}} - 5\delta\mathcal{J}_{\text{avg}}$, $J_{3z^2-r^2,xy} = J_{e_g}$, and $J_{x^2-y^2,xz} = J_{x^2-y^2,yz} = J_{t_{2g}}$; the orbital-diagonal direct exchange is $U_0 = U_{\text{avg}} + \frac{8}{5}\mathcal{J}_{\text{avg}}$. For some materials, we calculate the screened Coulomb integrals U_{avg} and \mathcal{J}_{avg} using the constrained local-density approximation (cLDA) approach.⁴³

We solve Hamiltonian (1) using different approaches. In Sec. III A we present exact diagonalization results (atomic limit). In Sec. III B we show results obtained with second-order perturbation theory (superexchange energy gain). In Sec. III C we present dynamical mean-field theory calculations within the LDA+DMFT (local-density approximation + dynamical mean-field theory) approach; for the latter we use a weak-coupling continuous-time quantum Monte Carlo⁴⁴ (CT-QMC) quantum-impurity solver and work with the full self-energy matrix in orbital space,^{40,45} as discussed in Ref. 46. We obtain the spectral-function matrix by means of stochastic reconstruction.⁴⁷ Since LDA+DMFT calculations for a five-band model with full Coulomb vertex⁴⁸ and self-energy matrix are computationally very expensive, a massively-parallel implementation as presented in Ref. 46 is essential. Structural data for LaCoO_3 are taken from Refs. 32 and 34, for YCoO_3 from Ref. 27, and for the other LnCoO_3 materials⁴⁹ from Refs. 50, 29, and 28. High-pressure data are from Ref. 23.

III. RESULTS

A. Atomic limit, Jahn-Teller, and constraints

1. Energies in the atomic limit

Let us examine the eigenstates of (1) in the atomic limit, i.e., in the limit $t_{m,m'}^{i,i'} = 0$ for $i \neq i'$ (see Fig. 2). The crystal-field states, the states which diagonalize the on-site matrix $t_{m,m'}^{i,i}$, have energy ε_α , with $\varepsilon_\alpha \leq \varepsilon_{\alpha+1}$; $\alpha = 1, 2, 3$ are t_{2g} -like states and $\alpha = 4, 5$ e_g like. In the atomic limit, the energy of the low-spin state (t_{2g}^6) is

$$E_L \sim 15U_0 - 30(\mathcal{J}_{\text{avg}} + \delta\mathcal{J}_{\text{avg}}) + 2 \sum_{\alpha \in t_{2g}} \varepsilon_\alpha.$$

The states with intermediate spin ($t_{2g}^5 e_g^1$) can be written as $|\alpha, \beta\rangle$, where α is the t_{2g} hole orbital and β the e_g electron orbital. The energy of the IS, in the limit in which only the density-density Coulomb terms contribute, is

$$E_I \sim E_L - 3\mathcal{J}_{\text{avg}} + (23 + f)\delta\mathcal{J}_{\text{avg}} + \Delta^{\text{JT}},$$

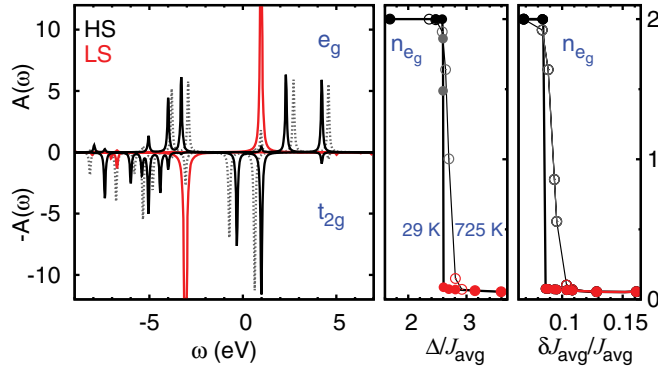


FIG. 2. (Color online) (Left) Atomic spectral functions at 29 K for different values of the ratio $\Delta/\mathcal{J}_{\text{avg}}$. (Black solid line) $\Delta/\mathcal{J}_{\text{avg}} \sim 1.69$. (Dotted line) $\Delta/\mathcal{J}_{\text{avg}} \sim 2.60$. (Gray solid line) $\Delta/\mathcal{J}_{\text{avg}} \sim 2.61$. Coulomb parameters: $U_{\text{avg}} = 3$ eV, $\mathcal{J}_{\text{avg}} = 0.89$ eV. (Center) Occupation of the e_g states as a function of $\Delta/\mathcal{J}_{\text{avg}}$ at low and high temperatures. (Right) Occupation of the e_g states as a function of $\delta\mathcal{J}_{\text{avg}}/\mathcal{J}_{\text{avg}}$ at low and high temperatures; the results are obtained for $\mathcal{J}_{\text{avg}} \sim 0.89$ eV, $\Delta/\mathcal{J}_{\text{avg}} \sim 2.64$ and varying F_4/F_2 in the interval $[0.1, 0.8]$.

where $\Delta^{\text{LI}} = \varepsilon_4 - \varepsilon_3$; the factor f yields the deviation from the average anisotropy of the exchange interaction; $f = -8$ for $|xy, x^2 - y^2\rangle$ and cyclic xyz permutations. The energy of a high-spin $t_{2g}^4 e_g^2$ is

$$E_H \sim E_L - 8\mathcal{J}_{\text{avg}} + 30\delta\mathcal{J}_{\text{avg}} + 2\Delta^{\text{LH}},$$

where $\Delta^{\text{LH}} = (\varepsilon_5 + \varepsilon_4 - \varepsilon_3 - \varepsilon_2)/2$. From the energy differences between the spin configurations we can obtain constraints for the parameters. Theoretical estimates⁵¹ yield $F_2 \sim 10.64$ eV and $F_4 \sim 6.8$ eV; with these values $\mathcal{J}_{\text{avg}} \sim 0.89$ eV and $\delta\mathcal{J}_{\text{avg}} \sim 0.07$ eV $\sim 0.08\mathcal{J}_{\text{avg}}$; other estimates⁵² yield slightly smaller values; by using cLDA we obtain $\mathcal{J}_{\text{avg}} \sim 0.7$ eV; furthermore, we find that \mathcal{J}_{avg} varies little when La is replaced by Eu in EuCoO_3 , a material which apparently exhibits no spin-state transition below the insulator-to-metal transition.²⁹ Since screened Coulomb exchange parameters can only be obtained within given approximations, we will discuss our results for a range of plausible values of \mathcal{J}_{avg} , ranging from 0.5 to 1 eV.

2. Cubic e_g - t_{2g} crystal-field splitting and Coulomb anisotropy

In Fig. 3 we show the calculated crystal-field splitting. We calculate the splittings in LaCoO_3 at ambient pressure and for increasing temperature,^{31,32} at room temperature for increasing pressure,^{23–26,53} and in the series of RCoO_3 compounds.^{27,50,54,55} Our results show that $\Delta^{\text{LH}} \sim 1.6$ – 1.7 eV in the full series,⁵⁶ while $\Delta^{\text{LI}} \sim 1.4$ – 1.6 eV. From these results we can derive the following conclusions. The ground state is LS if the following conditions are met:

$$\Delta^{\text{LH}} \gtrsim 4\mathcal{J}_{\text{avg}} - 15\delta\mathcal{J}_{\text{avg}} \sim 2.8\mathcal{J}_{\text{avg}},$$

$$\Delta^{\text{LI}} \gtrsim 3\mathcal{J}_{\text{avg}} - (23 + f)\delta\mathcal{J}_{\text{avg}} \sim 1.16\text{--}1.8\mathcal{J}_{\text{avg}},$$

where, for the second condition, we give the range varying f from 0 (average) to -8 ($|xy, x^2 - y^2\rangle$). Let us consider the cubic case ($\Delta^{\text{LH}} = \Delta^{\text{LI}} = \Delta_{\text{avg}} = \Delta$). In this case, the first condition is the most stringent. Exact diagonalization of the

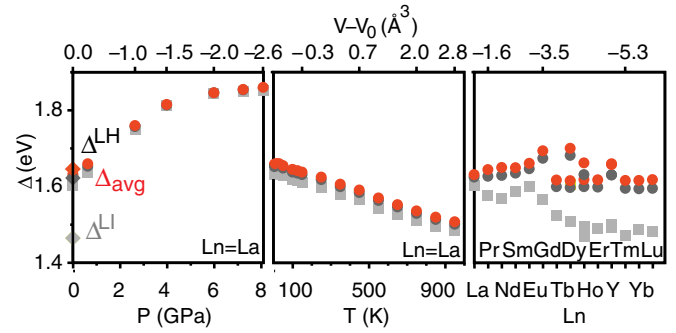


FIG. 3. (Color online) Crystal-field splittings as a function of pressure (left), temperature (center), and of the Ln ion (right). The corresponding volumes are also given; V_0 is the volume of LaCoO_3 at room temperature and ambient pressure. $\Delta^{\text{LI}} = \varepsilon_4 - \varepsilon_3$ (squares), $\Delta_{\text{avg}} = (\varepsilon_4 + \varepsilon_5)/2 - (\varepsilon_1 + \varepsilon_2 + \varepsilon_3)/3$ (dark circles), and $\Delta^{\text{LH}} = (\varepsilon_4 + \varepsilon_5)/2 - (\varepsilon_2 + \varepsilon_3)/2$ (light circles) are shown. In the cubic limit, $\Delta^{\text{LI}} = \Delta^{\text{LH}} = \Delta_{\text{avg}} = \Delta$. Multiple points for the same compound are results from different structural data sets.

atomic limit Hamiltonian with full exchange interaction and $\delta\mathcal{J}_{\text{avg}}/\mathcal{J}_{\text{avg}} \sim 0.08$ (Fig. 2) indeed leads to a switch between a high- and low-spin ground state at slightly smaller values, $\Delta \sim 2.6\mathcal{J}_{\text{avg}}$. From these results we conclude that, to explain a $S = 0$ ground state in the atomic limit, \mathcal{J}_{avg} must be slightly smaller than estimated with cLDA and similar approaches, $\mathcal{J}_{\text{avg}} \sim 0.6$ eV; alternatively, less likely, $\mathcal{J}_{\text{avg}} \sim 0.7$ eV but the anisotropy should be sizably larger than in the free atom,⁵⁷ $\delta\mathcal{J}_{\text{avg}} \sim 0.12\mathcal{J}_{\text{avg}}$. In any case, with the crystal-field splittings in Fig. 3, we are quite close to the HS/LS crossover. In this parameter region, the ~ 100 – 200 meV changes in crystal-field that we find (Fig. 3) with increasing temperature or pressure could indeed explain *alone* a spin-state crossover from LS to HS or vice versa. For a IS ground state, the following conditions should be met:

$$2\Delta^{\text{LH}} - \Delta^{\text{LI}} \gtrsim \left(5 - (7 - f)\frac{\delta\mathcal{J}_{\text{avg}}}{\mathcal{J}_{\text{avg}}}\right)\mathcal{J}_{\text{avg}} \sim 4.5\text{--}3.8\mathcal{J}_{\text{avg}}$$

$$\Delta^{\text{LI}} \leq 3\mathcal{J}_{\text{avg}} - (23 + f)\delta\mathcal{J}_{\text{avg}} \sim 1.16\text{--}1.8\mathcal{J}_{\text{avg}}.$$

This definitely excludes a IS ground state in the cubic case as, in all systems considered, the two conditions are never satisfied at the same time. For a LS \rightarrow IS scenario, it could be sufficient, however, that the IS state is lower than the HS (first condition). In the cubic case, for the parameters in Fig. 3, this could happen only for apparently unrealistically small Coulomb exchange \mathcal{J}_{avg} (~ 0.4 eV or smaller) or unrealistically large⁵⁷ anisotropy $\delta\mathcal{J}_{\text{avg}}/\mathcal{J}_{\text{avg}}$ (~ 0.16); in these cases the IS would, however, be quite high in energy (~ 1 eV or more) above the LS. Thus, the predictions of conventional ligand-field theory⁵⁸ are in agreement with our results for the atomic limit.

3. Jahn-Teller and other distortions

Let us analyze the effects of crystal distortions on the crystal-field splittings of e_g ($\Delta_{54} = \varepsilon_5 - \varepsilon_4$) and t_{2g} ($\Delta_{31} = \varepsilon_3 - \varepsilon_1$, $\Delta_{21} = \varepsilon_2 - \varepsilon_1$) states and the corresponding crystal-field orbitals. In Fig. 4 we show Δ_{54} , Δ_{31} , and Δ_{21} along

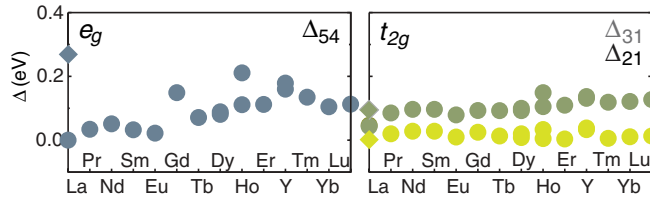


FIG. 4. (Color online) Crystal-field splitting (in eV) of e_g (left) and t_{2g} (right) states at room temperature as a function of decreasing ionic radius. Multiple points for the same compound are results from different structural data.^{27,50,54,55,59} LaCoO₃: $I2/a$ (diamonds) and $R\bar{3}c$ (circles).

the series; we find that the splitting of e_g states, Δ_{54} , reaches a maximum of 200 meV in HoCoO₃ and 250 meV in tetragonal³⁴ LaCoO₃, and is zero in rhombohedral LaCoO₃; furthermore, we find that Δ_{21} is small while Δ_{54} and Δ_{31} are comparable, the only exception being the $I2/a$ LaCoO₃ structure. Finally, across the spin-state transition, for available structural data, we find either basically no change in e_g and t_{2g} crystal-field splittings (LaCoO₃, $R\bar{3}c$) or a tiny change of 40 meV and no significant change in occupied orbital (YCoO₃). Even if we assume that the crystal-field splittings in Fig. 4 are completely ascribed to the Jahn-Teller effect, they are small compared to Jahn-Teller systems such as manganites or cuprates⁴⁵; they are comparable with splittings arising from the GdFeO₃-type distortion ($Pbnm$ structures)^{40,60} which progressively increase along the LnCoO₃ series.^{54,55} LaCoO₃ has to be discussed separately. While the presence of JT distortion is still controversial experimentally, even the monoclinic structure with cooperative Jahn-Teller distortion reported in Ref. 34 leads to a small splitting of e_g and t_{2g} states (see Fig. 4), although larger than for all other LnCoO₃ compounds considered here.

The splittings of e_g and t_{2g} states might affect the energy balance between spin states. To quantify this effect, we introduce the average splitting $\delta\Delta = (\Delta_{54} + \Delta_{31})/2$. Then, on the basis of Fig. 4, $\Delta^{\text{LH}} \sim \Delta$, $\Delta^{\text{LI}} \sim \Delta - \delta\Delta$. In the light of presently known structural data, remarkably, in the full LnCoO₃ series, $\delta\Delta$ is at most 150 meV, which is insufficient to lead to a LS-IS scenario, which would require $\delta\Delta \sim 1-1.7 \mathcal{J}_{\text{avg}}$ or larger. Such a scenario could perhaps start to play a role under high pressure, if $\delta\Delta$ sizably increases.

4. Final remarks

Our results show that the anisotropy $\delta\mathcal{J}_{\text{avg}}$ plays an important role in stabilizing the low-spin ground state (Fig. 2); if we neglect it ($J_1 = \mathcal{J}_{\text{avg}} = \mathcal{J}$), an approximation often adopted, the constraint for a low-spin ground state becomes $\Delta^{\text{LH}} > 4\mathcal{J}$. Thus, if the e_g - t_{2g} crystal-field splitting Δ has the values of Δ_{avg} in Fig. 3, the effective Coulomb exchange has to be as small as $\mathcal{J} \sim 0.4$ eV in order to obtain a LS ground state.⁶¹ On the other hand, if the anisotropy is unrealistically larger than for atomic orbitals, the IS state can become the first excited state. As a consequence, for systems close to spin-state transitions, differences in total energy between spin states might be extremely sensitive to the approximations adopted in describing the multiplet structure.^{3,63-65}

The value of U_{avg} does not affect the energy differences between spin-states in the atomic limit, but is relevant for the insulator-to-metal transition and the gap, as well as for superexchange. Theoretical estimates based on density-functional theory^{12,51,66} yield ~ 8 eV in LaCoO₃, and we find similar values with constrained LDA. Experimental estimates based on electron spectroscopy⁶⁷ yield sizably smaller values (~ 3.5 eV); similar values were adopted in many works.^{17,19,37} A configuration-interaction cluster model analysis of spectroscopic data yields $U_{\text{avg}} = 5.5$ eV for the low- and intermediate-spin states and ~ 6.8 eV for the high-spin state. Since the value of U_{avg} affects energy scales such as the size of the gap and superexchange, when necessary, in the next sections, we present results for several U_{avg} .

In conclusion, our results show that, in the atomic limit, for all systems analyzed, a LS \rightarrow IS scenario is unlikely. At close inspection, LDA+ U total-energy calculations are in line with this conclusion,^{12,17-19} as they indicate clearly that the stabilization of a given local magnetic state (IS or HS) strongly depends on the number and type of surrounding magnetic neighbors, suggesting that cooperative, band, or at least multisite effects play a crucial role; at low concentrations, in the absence of magnetic neighbors, the HS appears to be the favored magnetic state.^{1,17} Another important aspect is the evolution of the parameters with increasing temperature. For LaCoO₃ we find that the crystal field Δ_{avg} is reduced by about 150 meV when the temperature increases from 5 K to 1000 K. Remarkably, magnetic susceptibility data¹¹ indicate that the LS \rightarrow HS activation energy, Δ_{AE} , increases with temperature; similarly, the analysis of XAS data by means of the truncated configuration-interaction cluster approach³ suggests a rise of about 60 meV from 50 K to 700 K.¹¹ This result cannot be explained in the atomic limit, even including the effects of spin-orbit interaction, $\lambda\mathbf{S} \cdot \mathbf{L}$; we calculate the spin-orbit coupling λ for LaCoO₃ and find $\lambda \sim 54$ meV, slightly larger than the one assumed in model calculations,³⁶ but too small to affect the trends on Δ_{avg} . Our results also exclude that the rhombohedral distortions increase enough with temperature to overcome the decrease in Δ_{avg} due to the increasing volume.⁶⁸

B. Superexchange

Away from the atomic limit, superexchange affects the energy balance. However, is the superexchange energy gain large enough to be relevant in the spin-state crossover at T_{SS} ? In this section we calculate the superexchange energy gain for several types of Co-Co bonds: LS-LS, HS-HS, and LS-HS pairs; we do not consider IS-LS pairs, whose formation at low temperatures is unlikely.¹⁷ While differences in the energy of multiplets with a fixed number of electrons, relevant to determine the spin-state, are of the order \mathcal{J} , virtual excitations of electrons to neighboring sites, relevant for superexchange, involve the direct Coulomb energy U . Thus, the Coulomb exchange anisotropy $\delta\mathcal{J}_{\text{avg}}$ has a small effect on superexchange; for simplicity, we neglect it and consider density-density terms only. First, we consider the superexchange energy gain in the paramagnetic case. In a second step, we consider the effects of magnetic order.

1. Paramagnetic superexchange energy gain

For a LS-LS pair we obtain the (covalent) energy gain

$$\delta E_{SE}^{LS-LS} = - \sum_{\alpha=1}^3 \sum_{\alpha'=4}^5 \frac{|t_{\alpha',\alpha}^{i,i'}|^2 + |t_{\alpha,\alpha'}^{i,i'}|^2}{U_0 - 5\mathcal{J} + \Delta_{\alpha',\alpha}}, \quad (2)$$

where $\Delta_{\alpha',\alpha} = \varepsilon_{\alpha'} - \varepsilon_{\alpha}$. For a HS-HS pair, assuming that Co ions are in a paramagnetic state, we obtain

$$\delta E_{SE}^{HS-HS} = - \frac{1}{2n_{\beta}^2} \sum_{\{\beta\},\{\beta'\}} \left[\sum_{\alpha \neq \beta} \sum_{\alpha' \neq \beta'} \frac{|t_{\alpha,\alpha'}^{i,i'}|^2 + |t_{\alpha',\alpha}^{i,i'}|^2}{U_0 + 3\mathcal{J} + \Delta_{\alpha',\alpha}} + \sum_{\alpha' \neq \beta'} \frac{|t_{\beta,\alpha'}^{i,i'}|^2 + |t_{\alpha',\beta}^{i,i'}|^2}{U_0 - 3\mathcal{J} + \Delta_{\alpha',\beta}} + \frac{|t_{\beta,\alpha'}^{i,i'}|^2 + |t_{\alpha',\beta}^{i,i'}|^2}{U_0 + \mathcal{J} + \Delta_{\alpha',\beta}} \right],$$

where $\{\beta\}$ are the n_{β} degenerate t_{2g} levels, over which we average. Results for material-dependent hopping integrals are shown in Fig. 5. We find that for $U_{\text{avg}} \sim 5$ eV or larger the energy gains do not change much with increasing \mathcal{J} from 0 to 1 eV.⁶⁹ Instead, for fixed $\mathcal{J} \sim 0.89$ eV, we find a remarkable change in δE_{SE}^{LS-LS} reducing U_{avg} to ~ 3.5 eV, because the denominator sizably decreases. In Fig. 5 we show two significant parameter ranges. For $U_{\text{avg}} \sim 5.5$ eV, superexchange favors a high-spin ground state for LaCoO₃ for all temperatures and pressures considered. In the series LnCoO₃, the superexchange energy gain becomes larger for a LS ground state for ions smaller than Dy³⁺. For $U_{\text{avg}} \sim 3.5$ eV the crossing happens already for Ln = Sm, and the energy gain per LS-LS bond increases sizably to 90 meV around Ln = Y.

At this point it is crucial to evaluate also the superexchange energy gain associated with the formation of a HS-LS bond,

given by

$$\delta E_{SE}^{HS-LS} = - \frac{1}{2n_{\beta}} \sum_{\{\beta\}} \left[\sum_{\alpha \neq \beta} \sum_{\alpha'=4}^5 \frac{|t_{\alpha,\alpha'}^{i,i'}|^2 + |t_{\alpha',\alpha}^{i,i'}|^2}{U_0 - \mathcal{J} + \Delta_{\alpha',\alpha}} + \sum_{\alpha'=4}^5 \left(\frac{|t_{\beta,\alpha'}^{i,i'}|^2 + |t_{\alpha',\beta}^{i,i'}|^2}{U_0 - 7\mathcal{J} + \Delta_{\alpha',\beta}} + \frac{|t_{\beta,\alpha'}^{i,i'}|^2 + |t_{\alpha',\beta}^{i,i'}|^2}{U_0 - 3\mathcal{J} + \Delta_{\alpha',\beta}} \right) + \sum_{\alpha' \neq \beta} \sum_{\alpha=1}^3 \frac{|t_{\alpha,\alpha'}^{i,i'}|^2 + |t_{\alpha',\alpha}^{i,i'}|^2}{U_0 - \mathcal{J} + \Delta_{\alpha',\alpha}} \right]. \quad (3)$$

This energy gain is relevant in many scenarios of spin-state crossover. We find that $\delta E_{SE}^{HS-LS} / \delta E_{SE}^{HS-HS}$ is ~ 1.5 – 2 for $U_{\text{avg}} \sim 5.5$, and it increases with decreasing U_{avg} . Furthermore, all superexchange energy gains calculated here vary slowly with increasing temperature. These results show that, even neglecting lattice relaxation effects,¹ it is energetically favorable to form isolated HS ions rather than HS-HS bonds.

2. Effective Ising model

Here we present a simple model which accounts for the effects of superexchange discussed above, and the effects of lattice relaxation. The superexchange energy difference between a HS-HS and a LS-LS pair is

$$\delta E^{LH} = (\delta E_{SE}^{HS-HS} - \delta E_{SE}^{LS-LS}).$$

For $U_{\text{avg}} = 5.5$ eV, we find $\delta E^{LH} < 0$ (energy gain if a HS-HS is formed) for systems with a larger ionic radius and $\delta E^{LH} > 0$ (energy loss) for systems with a smaller ionic radius. The energy cost of a HS-HS pair with respect to two isolated HS ions is

$$\delta E_{SE}^{HH} \sim \delta E_{SE}^{HS-HS} + \delta E_{SE}^{LS-LS} - 2\delta E_{SE}^{HS-LS}.$$

We find that $\delta E_{SE}^{HH} > 0$ for all systems and all parameter ranges. For $U_{\text{avg}} = 5.5$ eV, it decreases from 70 to 30 meV along the series; for fixed Ln, it increases with decreasing U_{avg} . Based on these results, we can build a model which describes the system. We introduce pseudospin operators σ_z and identify LS sites with spin-down and HS sites with spin-up.⁷⁰ The interactions between spins yield an Ising-like model,

$$H_{\text{eff}} = \sum_i h(T) \sigma_z^i + \frac{1}{2} \sum_{\langle ji \rangle} \gamma \sigma_z^i \sigma_z^j.$$

Here $n_i = n_i^H + n_i^L = 1$ is the occupation per site, $\sigma_z^i = n_i^H - n_i^L$, and $\langle ji \rangle$ are near neighboring lattice sites. The parameter

$$h(T) = \frac{1}{2} E^{LH}(T) + \frac{1}{4} q \delta E^{LH},$$

where q is the coordination number, plays the role of an external field. The temperature enters explicitly only in

$$E^{LH}(T) = -3\mathcal{J}_{\text{avg}} + 30\delta\mathcal{J}_{\text{avg}} + 2\Delta^{LH}(T).$$

The coupling is $\gamma = \frac{1}{4} \delta E_{SE}^{HH} > 0$ (antiferro). In static mean field theory, a LS homogeneous state is given by the solution of the self-consistent equation

$$\langle \sigma_z^i \rangle = \tanh(-h(T) - q\gamma \langle \sigma_z^i \rangle) \beta.$$

At low temperatures, $h(T) > 0$ is large and the system is in a fully polarized ferro LS state. Increasing the temperature, $h(T)$

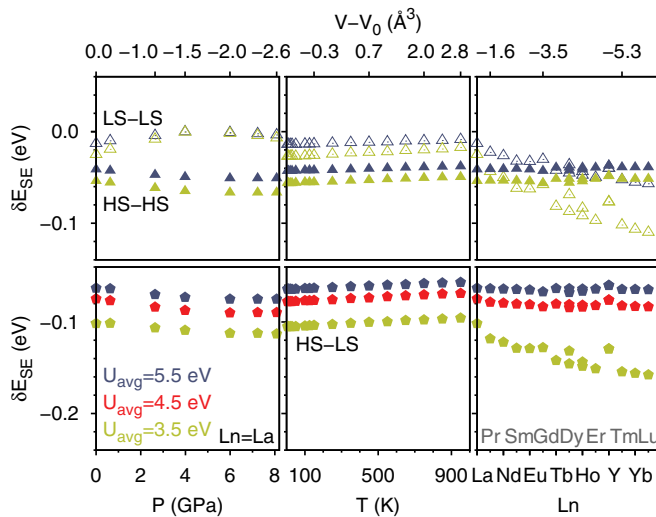


FIG. 5. (Color online) Superexchange energy gain per bond, δE_{SE} , for a LS-LS pair (empty triangles), a HS-HS pair (filled triangles), and a LS-HS pair (pentagons). (Left) δE_{SE} as a function of pressure. (Center) δE_{SE} as a function of temperature. (Right) δE_{SE} as a function of Ln ion. The corresponding volumes are also given; V_0 is the volume of LaCoO₃ at room temperature and ambient pressure. Multiple points for the same compound are results obtained starting from different structural data sets.

decreases linearly (Fig. 3), allowing the formation of some HS sites. We find that δE^{LH} increases with decreasing ionic radius; the crystal-field is instead maximum around Ln = Eu (Fig. 3). An increase of activation energy from 1200 K in LaCoO₃ to 3200 K in EuCoO₃ has been indeed reported.²⁹

When HS states form, covalency-driven lattice relaxation effects^{1,3} change the environment. In our model, if we take into account only two-site interactions, this effect enhances $\gamma \rightarrow \gamma' = \gamma + \gamma_{\text{rel}}$, thus favoring a AF HS/LS phase, described in mean field by

$$\langle \sigma_z^i \rangle = \tanh(-h(T) + q\gamma' \langle \sigma_z^i \rangle) \beta.$$

An overestimate of γ_{rel} can be obtained by using the difference between HS and LS in empirical ionic radii ($\delta r_{\text{IR}} \sim 0.06 \text{ \AA}$) and the fact that Δ varies linearly when changing the Co-O distance by a small amount; we can estimate the slope from our results (Fig. 3). We find $\gamma_{\text{rel}} \sim \frac{1}{4} 2\delta\Delta$, with $2\delta\Delta \sim \frac{1}{4} 2\Delta' \delta r_{\text{IR}} \sim 90 \text{ meV}$, decreasing to 80 meV at high temperatures, i.e., comparable with the superexchange term $\delta E_{\text{SE}}^{\text{HH}}$.

If $h(T) = 0$, eventually an antiferro ordered HS+LS lattice forms; the critical temperature for such a state can be estimated using mean-field theory, $k_B T_{\text{HS+LS}} = q\gamma'$. If $\gamma_{\text{rel}} = 0$, for $U_{\text{avg}} = 5.5 \text{ eV}$ $T_{\text{HS+LS}} \sim 1200 \text{ K}$ for Ln = La, decreasing to 500 K for Ln = Lu; γ_{rel} enhances $T_{\text{HS+LS}}$ of about 1300 K.

The critical temperatures we obtain are very large. However, although $h(T) \rightarrow 0$ with increasing temperature, it likely remains comparable to γ' to very high temperatures; thus, the lattice stays disordered and perhaps even close to a LS ferro solution in a large temperature range, with $\langle \sigma_z^i \rangle$ (i.e., the occupation of LS states) decreasing linearly with increasing temperature. Indeed, in LaCoO₃ it has been reported that the fraction of HS sites rises slowly from 0.1 to 0.4 increasing the temperature from 100 to 700 K.³ Hysteresis effects could arise because of the lattice relaxation.

3. Magnetic superexchange

Up to here we have assumed that in HS-HS pairs Co HS ions stay paramagnetic and paraorbital. However, a specific molecular state could form as well as a spin singlet or triplet. We find that orbitals in the degenerate t_{2g} states play a minor role, because the energy differences of different orbital states with respect to the orbital average is small. Instead, the formation of a magnetic singlet could play a role. In order to estimate the associated energy gain, we calculated the coupling constant Γ_{SE} of the Heisenberg interaction $\Gamma_{\text{SE}} \mathbf{S}_i \cdot \mathbf{S}_j$ for a HS pair. We find that Γ_{SE} is AFM for all systems (see Fig. 6). In LaCoO₃, for $U_{\text{avg}} = 5.5 \text{ eV}$, we find $\Gamma_{\text{SE}} \sim 7 \text{ meV}$ at room temperature and ambient pressure; it increases to 10 meV if the pressure rises to 8 GPa and slightly decreases with increasing temperature. Reducing the ionic radius the anisotropy of Γ_{SE} increases, but the average magnetic coupling decreases down to 8 meV for Ln = Lu. Next we assume that in all systems, due to the spin-orbit coupling, the effective magnetic moment $p = \sqrt{J(J+1)} \sim \sqrt{2}$; then, the magnetic energy gain associated with the formation of a singlet is $-\frac{9}{4}\Gamma_{\text{SE}}$, which in LaCoO₃ is $\sim -18 \text{ meV}$. This energy gain partially reduces $\delta E_{\text{SE}}^{\text{HH}}$ and, therefore, γ , which would change sign around the end of the series if $U_{\text{avg}} \sim 5.5 \text{ eV}$; however, $\delta E_{\text{SE}}^{\text{HH}}$ increases

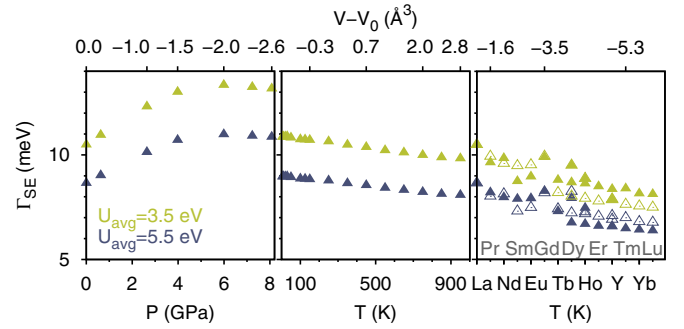


FIG. 6. (Color online) Magnetic coupling Γ_{SE} for a HS-HS pair, as a function of pressure (left), temperature (center), and of Ln ion [right; open symbols: (001) direction; solid symbols: (100) or (010) direction]. The corresponding volumes are also given; V_0 is the volume of LaCoO₃ at room temperature and ambient pressure. Multiple points for the same compound are results from different structural data sets.

rapidly with decreasing U_{avg} . The smaller $T_{\text{HS+LS}}$ is, the more favorable is a disordered phase, reinforcing the conclusions of the paragraph above.

However, the magnetic coupling Γ_{SE} is sizable, and magnetic interactions would be crucial in a homogeneous HS-HS state. In mean-field theory, the critical temperature $T_N \sim \frac{9}{4}\Gamma_{\text{SE}} J(J+1)$ should then be $\sim 500 \text{ K}$ for LaCoO₃, decreasing in the series to 400 K and increasing under pressure to about 700 K. The mean-field values are overestimates; quantum-fluctuation effects, further crystal-field splittings reducing the effective magnetic moment, and the zero-field splitting reduce T_N . Still, even taking reduction factors into account, many cobaltates, if in a homogeneous HS state, should be magnetic because the spin-state transition occurs at $T_{\text{SS}} < T_N$; in the presence of lonely HS-HS pairs, antiferromagnetic short-range correlations could be detected. On the other hand, if the number of ions thermally excited to a HS state is small to high temperatures and the phase is disordered, weak FM short-range correlations, as reported in dynamic neutron-scattering experiments, could perhaps be triggered by a double-exchange-like mechanism,⁵¹ or even alone by the small but finite zero-field splitting.¹¹

C. High-temperature phase

The transition observed at T_{IM} is usually ascribed to a semiconductor-to-metal transition, the nature of which is hotly debated. There are indications that strong correlations play a crucial role and that the spin-state transition is also a crossover from a spin-gapped insulator to a Mott insulator.^{8,71} In the absence of firm evidence of the formation of superlattices, we analyze to what extent the insulator-to-metal transition can be understood in terms of a Mott transition within the homogeneous phase. Several works indeed suggest that the high-temperature phase could be a metallic homogeneous IS state.^{17,22} To clarify if this can be the case, we solve the Hamiltonian (1) by means of the LDA+DMFT approach⁷²; we perform calculations for LaCoO₃ (Figs. 7 and 8), for which spectral properties are best known. The experimental gap is $\sim 0.2 \text{ eV}$ at low temperatures and slightly larger ($\sim 0.5 \text{ eV}$)

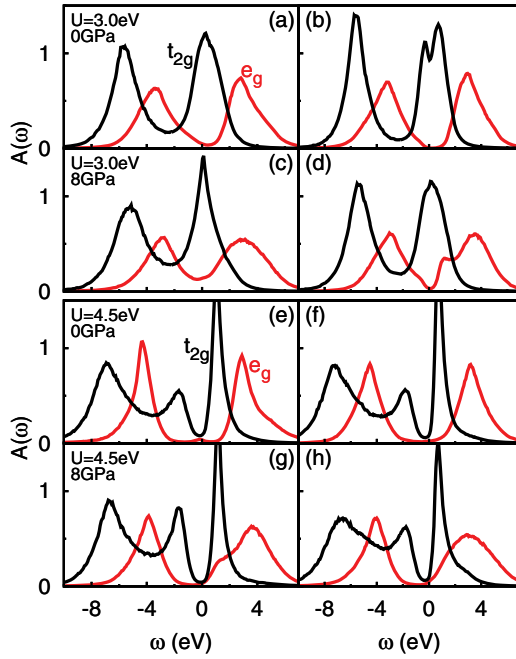


FIG. 7. (Color online) LaCoO_3 : Orbital-dependent spectral functions $A(\omega)$ calculated with LDA+DMFT for decreasing temperature, approaching the insulator-to-metal transition from above ($T/T_{\text{IM}} \sim 4 \rightarrow 2$). The spectral function is shown for the t_{2g} (black lines) and e_g electrons (gray lines), at $T/T_{\text{IM}} \sim 4$ [left column, panels (a), (c), (e), and (g)], and $T/T_{\text{IM}} \sim 2$ [right column, panels (b), (d), (f), and (h)]. The upper panels show the results for $U = U_{\text{avg}} = 3$ eV, $P = 0$ GPa [(a) and (b)] and 8 GPa [(c) and (d)] and the lower panels for $U = U_{\text{avg}} = 4.5$ eV, $P = 0$ GPa [(e) and (f)] and 8 GPa [(g) and (h)].

above 300 K; to be consistent with experimental gaps, we vary U_{avg} between 3 and 5 eV.

Figure 7 shows the LDA+DMFT results for $U_{\text{avg}} = 3$ eV and the ambient pressure structure for temperatures approaching T_{IM} [Figs. 7(a) and 7(b)]. We find a homogeneous high-spin state; thus, we do not find support for the proposed^{17,22} homogeneous IS state at high-temperature. Remarkably, we find metallic t_{2g} and insulating e_g spectral functions, i.e., an *orbital-selective* Mott state. This can be understood from the fact the t_{2g} electrons have a larger orbital degeneracy,⁷³ although a smaller bandwidth (Fig. 9), while the e_g electrons are half-filled in the HS state, and, therefore, the exchange

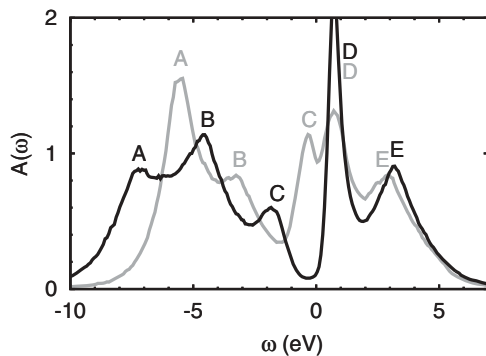


FIG. 8. Total LDA+DMFT spectral function ($T/T_{\text{IM}} \sim 3$) for LaCoO_3 ; $U_{\text{avg}} = 3$ eV (gray) and $U_{\text{avg}} = 4.5$ eV (black).

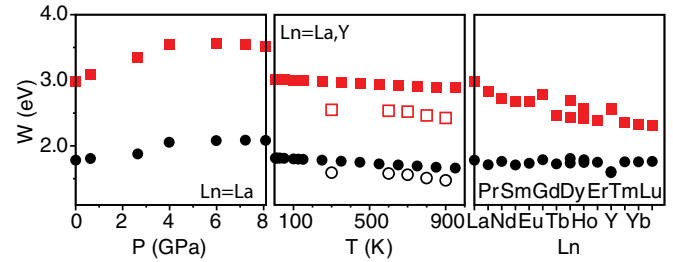


FIG. 9. (Color online) LnCoO_3 series: Evolution of the e_g (squares) and t_{2g} (circles) bandwidth with pressure ($\text{Ln} = \text{La}$, $R\bar{3}c$ structure), temperature (solid symbols: $\text{Ln} = \text{La}$ ($R\bar{3}c$ structure), and open symbols: $\text{Ln} = \text{Y}$), and ionic radius Ln^{3+} (right panel).

coupling \mathcal{J}_{avg} effectively enhances the Coulomb repulsion. Decreasing the temperature towards T_{IM} , a pseudogap opens in the e_g spectral-function, and eventually an insulating regime with a small gap and a corresponding bad metal behavior appears. We find that the multiplet positions in the spectral function are close to the atomic limit high-spin curve in Fig. 2. We repeat the calculation for the 8-GPa structure [Figs. 7(c) and 7(d)]; this system has a larger crystal-field Δ_{avg} , very close, for the chosen exchange parameters, to the low-spin-to-high-spin ground-state crossover in the atomic limit. Compared to the ambient pressure case, the e_g gap is smaller, while, at fixed temperature, the t_{2g} spectral function remains metallic with higher low-energy density of states. These results indicate that, as far as the state remains HS, at 8 GPa the insulator-to-metal transition should occur at lower temperatures than at ambient pressure, i.e., the system should stay metallic. Experiments show, however, that LaCoO_3 returns to the insulating state under pressure.^{24,26} Our results exclude that this can happen in a HS scenario and are instead compatible with the suggestion²⁴ that the metal-insulator transition observed under pressure is driven by a spin-state transition.

Increasing U_{avg} to ~ 4.5 eV we find [Figs. 7(e), 7(f), 7(g), and 7(h)] that a real gap opens in the t_{2g} spectral function and both e_g and t_{2g} spectral functions are insulating, even at high temperatures. The t_{2g} gap is small, still compatible with the bad metal behavior observed for $T > T_{\text{IM}}$. Furthermore, calculations for the high-pressure structure show that the t_{2g} spectral function does not change much while the e_g gap is reduced. This can be understood by observing that the e_g bandwidth increases substantially more than the t_{2g} bandwidth increasing pressure (Fig. 9).

The total spectral function at ambient pressure is shown in Fig. 8. We find three negative energy peaks (A, B, and C) and two positive energy features (D and E). For $U_{\text{avg}} \sim 4.5$ eV, peak A is at -7.5 eV, peak B is at -4.7 eV, ~ 2 eV above, and peak C is at ~ -1.9 eV, features all observed in XPS, UPS, or photoemission data.^{10,37,67,74} The spectra for $U_{\text{avg}} = 3$ eV and $U_{\text{avg}} = 4.5$ eV differ in particular in the photoemission part; reducing U_{avg} to 3 eV, we find that the spectrum is moved almost rigidly toward the right by about 2 eV; the first and second features move to -5.5 and -3.5 eV respectively, while the lowest energy peak moves to -0.5 eV, very close to the Fermi edge, to partially merge with the 0.8-eV peak. Finally, spectral weight moves from B to C and A. While the exact positions of peaks A, B, and C shift with U_{avg} , the overall

shape of the spectral function appears in line with XPS, BIS, XAS, and PES data at room temperature.^{67,74,75} The positive energy features D and E at ~ 1 eV and ~ 3 eV are reflected in the form of the XAS and BIS spectra.⁶⁷

Thus, the insulator-to-metal transition, as described in a homogeneous scenario, and the spin-state crossover exhibit different trends; the spin-state crossover is controlled by small changes in Δ , exchange anisotropy, and superexchange, parameters which change sizably with decreasing ionic radius. If the homogeneous HS is populated, a Mott-insulator-to-bad-metal transition can occur, at a temperature which depends strongly on the t_{2g} bandwidth and crystal fields.

IV. CONCLUSIONS

We have studied the nature of the spin-state and metal-insulator transition in LnCoO₃ cobaltates. We show that a low-temperature intermediate-spin-state scenario is unlikely in the full LnCoO₃ series. We show that the spin-state transition is controlled not only by the cubic crystal-field Δ and the

average Coulomb exchange \mathcal{J}_{avg} but, surprisingly, also by the Coulomb exchange anisotropy $\delta\mathcal{J}_{\text{avg}}$ and by superexchange. We propose a simple Ising-like model to describe the spin-state transition. We find that lattice relaxation and superexchange yield antiferro coupling of the same order, which competes with the crystal field. Our model qualitatively explains the trends observed in spin-state transitions in the LnCoO₃ series. By using the LDA+DMFT approach, we show that in LaCoO₃ a high-temperature homogeneous intermediate spin state is unlikely. Within a homogeneous HS state, we find that the HS metal-insulator transition has a different nature than the spin-state transition, as it mostly depends on the t_{2g} states and it could be orbital selective.

ACKNOWLEDGMENTS

We acknowledge discussions with H. Tjeng. Calculations were done on the Jülich Blue Gene/P and Juropa. We acknowledge financial support from the Deutsche Forschungsgemeinschaft through research unit FOR1346.

-
- ¹J. B. Goodenough, *J. Phys. Chem. Solids* **6**, 287 (1958); P. M. Raccah and J. B. Goodenough, *Phys. Rev. B* **155**, 932 (1967); J. B. Goodenough, *Mater. Res. Bull.* **6**, 967 (1971); M. A. Senaris-Rodriguez and J. B. Goodenough, *J. Solid State Chem.* **116**, 224 (1995).
- ²V. G. Bhide, D. S. Rajoria, G. Rama Rao, and C. N. R. Rao, *Phys. Rev. B* **6**, 1021 (1972).
- ³M. W. Haverkort, Z. Hu, J. C. Cezar, T. Burnus, H. Hartmann, M. Reuther, C. Zobel, T. Lorenz, A. Tanaka, N. B. Brookes, H. H. Hsieh, H.-J. Lin, C. T. Chen, and L. H. Tjeng, *Phys. Rev. Lett.* **97**, 176405 (2006).
- ⁴A. Podlesnyak, S. Streule, J. Mesot, M. Medarde, E. Pomjakushina, K. Conder, A. Tanaka, M. W. Haverkort, and D. I. Khomskii, *Phys. Rev. Lett.* **97**, 247208 (2006).
- ⁵N. Sundaram, Y. Jiang, I. E. Anderson, D. P. Belanger, C. H. Booth, F. Bridges, J. F. Mitchell, Th. Proffen, and H. Zheng, *Phys. Rev. Lett.* **102**, 026401 (2009).
- ⁶G. Thorthon, B. C. Tofield, and D. E. Williams, *Solid State Commun.* **44**, 1213 (1982); *J. Phys. Solid State Phys.* **21**, 2871 (1988).
- ⁷K. Asai, P. Gehring, H. Chou, and G. Shirane, *Phys. Rev. B* **40**, 10982 (1989).
- ⁸S. Yamaguchi, Y. Okimoto, H. Taniguchi, and Y. Tokura, *Phys. Rev. B* **53**, R2926 (1996).
- ⁹R. H. Potze, G. A. Sawatzky, and M. Abbate, *Phys. Rev. B* **51**, 11501 (1995).
- ¹⁰T. Saitoh, T. Mizokawa, A. Fujimori, M. Abbate, Y. Takeda, and M. Takano, *Phys. Rev. B* **55**, 4257 (1997).
- ¹¹S. Noguchi, S. Kawamata, K. Okuda, H. Nojiri, and M. Motokawa, *Phys. Rev. B* **66**, 094404 (2002).
- ¹²M. A. Korotin, S. Yu. Ezhov, I. V. Solovyev, V. I. Anisimov, D. I. Khomskii, and G. A. Sawatzky, *Phys. Rev. B* **54**, 5309 (1996).
- ¹³R. F. Klie, J. C. Zheng, Y. Zhu, M. Varela, J. Wu, and C. Leighton, *Phys. Rev. Lett.* **99**, 047203 (2007).
- ¹⁴C. Zobel, M. Kriener, D. Bruns, J. Baier, M. Grüninger, and T. Lorenz, P. Reutler, and A. Revcolevschi, *Phys. Rev. B* **66**, 020402 (2002).
- ¹⁵A. Ishikawa, J. Nohara, and S. Sugai, *Phys. Rev. Lett.* **93**, 136401 (2004).
- ¹⁶K. Asai, A. Yoneka, O. Yokokura, J. M. Tranquada, G. Shirane, and K. Kohn, *J. Phys. Soc. Jpn.* **67**, 290 (1998).
- ¹⁷K. Knížek, Z. Jirák, J. Hejtmanek, P. Novák, and W. Ku, *Phys. Rev. B* **79**, 014430 (2009).
- ¹⁸M. Zhuang, W. Zhang, and N. Ming, *Phys. Rev. B* **57**, 10705 (1998).
- ¹⁹K. Knížek, Z. Jirák, J. Hejtmanek, and P. Novák, *J. Phys.: Condens. Matter* **18**, 3285 (2006).
- ²⁰A. Laref and W. Sekkal, *Mater. Chem. Phys.* **123**, 125 (2010).
- ²¹J. Kunes and V. Křápek, *Phys. Rev. Lett.* **106**, 256401 (2011).
- ²²T. Kyomen, Y. Asaka, and M. Itoh, *Phys. Rev. B* **71**, 024418 (2005).
- ²³T. Vogt, J. A. Hriljac, N. C. Hyatt, and P. Woodward, *Phys. Rev. B* **67**, 140401(R) (2003).
- ²⁴R. Lengsdorf, J.-P. Rueff, G. Vankó, T. Lorenz, L. H. Tjeng, and M. M. Abd-Elmeguid, *Phys. Rev. B* **75**, 180401 (2007); R. Lengsdorf, M. Ait-Tahar, S. S. Saxena, M. Ellerby, D. I. Khomskii, H. Micklitz, T. Lorenz, and M. M. Abd-Elmeguid, *ibid.* **69**, 140403 (2004).
- ²⁵G. Vankó, J.-P. Rueff, A. Mattila, Z. Németh, and A. Shukla, *Phys. Rev. B* **73**, 024424 (2006).
- ²⁶D. P. Kozlenko, N. O. Golosova, Z. Jirák, L. S. Dubrovinsky, B. N. Savenko, M. G. Tucker, Y. Le Godec, and V. P. Glazkov, *Phys. Rev. B* **75**, 064422 (2007).
- ²⁷A. Mehta, R. Berliner, and R. W. Smith, *J. Solid State Chem.* **130**, 192 (1997); K. Knížek, Z. Jirák, J. Hejtmanek, M. Veverka, M. Maryško, B. C. Hauback, and H. Fjellvåg, *Phys. Rev. B* **73**, 214443 (2006).
- ²⁸J.-Q. Yan, J.-S. Zhou, and J. B. Goodenough, *Phys. Rev. B* **69**, 134409 (2004).
- ²⁹J. Baier, S. Jodlauk, M. Kriener, A. Reichl, C. Zobel, H. Kierspel, A. Freimuth, and T. Lorenz, *Phys. Rev. B* **71**, 014443 (2005).
- ³⁰K. Knížek, Z. Jirák, J. Hejtmanek, M. Veverka, M. Maryško, G. Maris, and T. T. M. Palstra, *Eur. Phys. J. B* **47**, 213 (2005).
- ³¹G. Thornton, B. C. Tofield, and A. W. Hewat, *J. Solid State Chem.* **61**, 301 (1986).
- ³²P. G. Radaelli and S.-W. Cheong, *Phys. Rev. B* **66**, 094408 (2002).

- ³³S. Xu, Y. Morimoto, K. Mori, T. Kamiyama, T. Saitoh, and A. Nakamura, *J. Phys. Soc. Jpn.* **70**, 3296 (2001).
- ³⁴G. Maris, Y. Ren, V. Volotchaev, C. Zobel, T. Lorenz, and T. T. M. Palstra, *Phys. Rev. B* **67**, 224423 (2003).
- ³⁵D. Louca, J. L. Sarrao, J. D. Thompson, H. Röder, and G. H. Kwei, *Phys. Rev. B* **60**, 10378 (1999); D. Louca and J. L. Sarrao, *Phys. Rev. Lett.* **91**, 155501 (2003).
- ³⁶R. Radwanski and Z. Ropka, *Solid State Commun.* **112**, 621 (1999); *Physica B* **281–282**, 507 (2000); Z. Ropka and R. Radwanski, *Phys. Rev. B* **67**, 172401 (2003).
- ³⁷S. K. Pandey, A. Kumar, S. Patil, V. R. R. Medicherla, R. S. Singh, K. Maiti, D. Prabhakaran, A. T. Boothroyd, and A. V. Pimpale, *Phys. Rev. B* **77**, 045123 (2008).
- ³⁸P. Blaha, K. Schwarz, G. Madsen, D. Kvasnicka, and J. Luitz, WIEN2K, *An Augmented Plane Wave + Local Orbitals Program for Calculating Crystal Properties* (Technische Universität Wien, Austria, 2001).
- ³⁹A. A. Mostofi, J. R. Yates, Y.-S. Lee, I. Souza, D. Vanderbilt, and N. Marzari, *Comput. Phys. Commun.* **178**, 685 (2008); J. Kunes, R. Arita, P. Wissgott, A. Toschi, H. Ikeda, and K. Held, *ibid.* **181**, 1888 (2010).
- ⁴⁰E. Pavarini, S. Biermann, A. Poteryaev, A. I. Lichtenstein, A. Georges, and O. K. Andersen, *Phys. Rev. Lett.* **92**, 176403 (2004); E. Pavarini, A. Yamasaki, J. Nuss, and O. K. Andersen, *New J. Phys.* **7**, 188 (2005).
- ⁴¹E. Pavarini, in *The LDA+DMFT Approach to Strongly Correlated Materials*, edited by E. Pavarini, E. Koch, A. Lichtenstein, and D. Vollhardt (Verlag des Forschungszentrum Jülich, Jülich, 2011).
- ⁴²Our parameters are related to the Racah parameters A , B , C by the following equations: $A = U_{\text{avg}} - \frac{7}{5}[\mathcal{J}_{\text{avg}} - 5\delta\mathcal{J}_{\text{avg}}]$, $B = 2\delta\mathcal{J}_{\text{avg}}$, $C = \mathcal{J}_{\text{avg}} - 5\delta\mathcal{J}_{\text{avg}}$. Thus, $\delta\mathcal{J}_{\text{avg}} = B/2$, $\mathcal{J}_{\text{avg}} = 5B/2 + C$, and $U_{\text{avg}} = A + 7C/5$, while $U_0 = A + 4B + 3C$. Notice that \mathcal{J}_{avg} is also the Kanamori parameter J , while U_0 is the Kanamori parameter U .
- ⁴³O. Gunnarsson, O. K. Andersen, O. Jepsen, and J. Zaanen, *Phys. Rev. B* **39**, 1708 (1989).
- ⁴⁴A. N. Rubtsov, V. V. Savkin, and A. I. Lichtenstein, *Phys. Rev. B* **72**, 035122 (2005).
- ⁴⁵E. Pavarini, E. Koch, and A. I. Lichtenstein, *Phys. Rev. Lett.* **101**, 266405 (2008); E. Pavarini and E. Koch, *ibid.* **104**, 086402 (2010); A. Flesch, G. Zhang, E. Koch, and E. Pavarini, *Phys. Rev. B* **85**, 035124 (2012).
- ⁴⁶E. Gorelov, M. Karolak, T. O. Wehling, F. Lechermann, A. I. Lichtenstein, and E. Pavarini, *Phys. Rev. Lett.* **104**, 226401 (2010); M. Malvestuto, E. Carleschi, R. Fittipaldi, E. Gorelov, E. Pavarini, M. Cuoco, Y. Maeno, F. Parmigiani, and A. Vecchione, *Phys. Rev. B* **83**, 165121 (2011).
- ⁴⁷A. S. Mishchenko, N. V. Prokof'ev, A. Sakamoto, and B. V. Svistunov, *Phys. Rev. B* **62**, 6317 (2000).
- ⁴⁸In order to reduce the computational effort, most calculations are performed keeping only density-density terms; we find that differences due to the neglected terms are small in the relevant parameter regime.
- ⁴⁹We find that the parameters depend very weakly on the position of $R4f$ levels; we obtain very similar results if we treat f electrons within LDA+ U ($U \in [0,7]$ eV), or if we replace R^{3+} with La^{3+} (empty $4f$ shell).
- ⁵⁰X. Liu and C. Prewitt, *J. Phys. Chem. Solids* **52**, 441 (1991); J. Pérez-Cacho, J. Blasco, J. García, and R. Sanchez, *J. Solid State Chem.* **150**, 145 (2000).
- ⁵¹R. Eder, *Phys. Rev.* **81**, 035101 (2010).
- ⁵²T. Mizokawa and A. Fujimori, *Phys. Rev. B* **54**, 5368 (1996).
- ⁵³E. Pavarini, S. C. Tarantino, T. B. Ballaran, M. Zema, P. Ghigna, and P. Carretta, *Phys. Rev. B* **77**, 014425 (2008).
- ⁵⁴J. A. Alonso, M. J. Martínez-Lope, C. de la Callea, and V. Pomjakushin, *J. Mater. Chem.* **16**, 1555 (2006).
- ⁵⁵K. Knížek, J. Hejtmánek, Z. Jiráček, P. Tomeš, P. Henry, and G. André, *Phys. Rev. B* **79**, 134103 (2009).
- ⁵⁶The crystal-field splittings obtained with the NMTO approach are slightly larger, but the trends remain the same. In the low-temperature ambient pressure phases $\Delta \sim 2.15$ eV while $\Delta \sim 2.4$ eV under a pressure of 8 GPa and ~ 2.05 eV at 900 K. For YCoO_3 we find ~ 2.15 eV at 300 K and 2.0 at ~ 900 K. The change in crystal-field splitting between high-spin and low-spin phases is, in all cases, at most 300 meV.
- ⁵⁷For $3d$ elements, the ratio F_4/F_2 is usually approximated to ~ 0.625 ; this yields $\delta\mathcal{J}_{\text{avg}}/\mathcal{J}_{\text{avg}} \sim 0.08$. The extreme values for $\delta\mathcal{J}_{\text{avg}}/\mathcal{J}_{\text{avg}}$ are 0 ($F_4 = F_2$) and 0.2 ($F_4 = 0$).
- ⁵⁸B. N. Figgis and M. A. Hitchman, in *Ligand Field Theory and Its Applications* (Wiley, New York, 2000).
- ⁵⁹G. Thornton, F. C. Morrison, S. Partington, B. C. Tofield, and D. E. Williams, *J. Phys. C* **21**, 2871 (1988); K. Knížek, Z. Jiráček, J. Hejtmánek, M. Veverka, M. Maryško, G. Maris, and T. T. M. Palstra, *Eur. Phys. J. B* **47**, 213 (2005).
- ⁶⁰M. De Raychaudhury, E. Pavarini, and O. K. Andersen, *Phys. Rev. Lett.* **99**, 126402 (2007).
- ⁶¹Notice that the simplification of the Coulomb vertex introduced in Ref. 62 and often successfully used in LDA+ U calculations, in the case of cobaltates leads to quite different multiplets than the actual Coulomb interaction. For example, the constraint for a LS ground state becomes $\Delta \geq 2J_{\text{avg}}$ and the energy difference between HS and IS state is $-3J_{\text{avg}} + \Delta$. Finally, in the extreme approximation in which only the spherically averaged Coulomb interaction is used, even the competition between Hund's rule coupling and crystal field is lost, except for the contribution coming from the exchange-correlation functional.
- ⁶²S. L. Dudarev, G. A. Botton, S. Y. Savrasov, C. J. Humphreys, and A. P. Sutton, *Phys. Rev. B* **57**, 1505 (1998).
- ⁶³T. Mizokawa and A. Fujimori, *Phys. Rev. B* **54**, 5368 (1996).
- ⁶⁴M. Takahashi and J.-I. Igarashi, *Phys. Rev. B* **55**, 13557 (1997).
- ⁶⁵See also H. Wu and T. Burnus, *Phys. Rev. B* **80**, 081105 (2009); H. Wu, *ibid.* **81**, 115127 (2010) for layered cobaltates.
- ⁶⁶H. Hsu, K. Umemoto, M. Cococcioni, and R. Wentzcovitch, *Phys. Rev. B* **79**, 125124 (2009).
- ⁶⁷A. Chainani, M. Mathew, and D. D. Sarma, *Phys. Rev. B* **46**, 9976 (1992).
- ⁶⁸C. S. Naiman, R. Gilmore, B. DiBartolo, A. Linz, and R. Santoro, *J. Appl. Phys.* **36**, 1044 (1965).
- ⁶⁹We find that, for \mathcal{J}_{avg} between 0 and 1 eV, the superexchange energy gain is reduced of about 30 meV for $S = 2$ and increased of about the same amount for $S = 0$; the trends remain the same.
- ⁷⁰The IS state could be included in our model as a third excited state. In this case, instead of a Ising model for a pseudospin 1/2, we would obtain an Ising model for a pseudospin 1.
- ⁷¹Y. Tokura, Y. Okimoto, S. Yamaguchi, H. Taniguchi, T. Kimura, and H. Takagi, *Phys. Rev. B* **58**, 1699 (1998).
- ⁷²To reduce the sign problem we dropped Coulomb terms without a density-density matrix form; this moves the spin-state transition to slightly larger values of Δ^{LH} ($2.8\mathcal{J}_{\text{avg}}$ versus $2.6\mathcal{J}_{\text{avg}}$), as discussed in Sec. II A, but do not affects the conclusions.

⁷³O. Gunnarsson, E. Koch, and R. M. Martin, *Phys. Rev. B* **56**, 1146 (1997); E. Koch, O. Gunnarsson, and R. M. Martin, *ibid.* **60**, 15714 (1999).

⁷⁴A. G. Thomas, W. R. Flavell, P. M. Dunwoody, C. E. J. Mitchell, S. Warren, S. C. Grice, P. G. D. Marr, D. E. Jewitt, N. Khan, V. R.

Dhanak, D. Teehan, E. A. Seddon, K. Asai, Y. Koboyashi, and N. Yamada, *J. Phys.: Condens. Matter* **12**, 9259 (2000).

⁷⁵M. Medarde, C. Dallera, M. Grioni, J. Voigt, A. Podlesnyak, E. Pomjakushina, K. Conder, Th. Neisius, O. Tjénberg, and S. N. Barilo, *Phys. Rev. B* **73**, 054424 (2006).